Neuron 51, 741–754, September 21, 2006 ©2006 Elsevier Inc. DOI 10.1016/j.neuron.2006.09.003

Neuroligins Determine Synapse Maturation and Function

Frédérique Varoqueaux,[1,8] Gayane Aramuni,[2,8] Randi L. Rawson,[1] Ralf Mohrmann,[3,4] Markus Missler,[2,5,6] Kurt Gottmann,[1,3,7] Weiqi Zhang,[2] Thomas C. Südhof,[5,*] and Nils Brose[1,5,*]

[1] Department of Molecular Neurobiology and Center for the Molecular Physiology of the Brain Max Planck Institute of Experimental Medicine D-37075 Göttingen Germany

[2] Center for Physiology and Pathophysiology and Center for the Molecular Physiology of the Brain Georg August University Göttingen D-37073 Göttingen Germany

[3] Department of Cell Physiology ND4 Ruhr University Bochum D-44780 Bochum Germany

[4] Department of Membrane Biophysics Max Planck Institute of Biophysical Chemistry D-37077 Göttingen Germany

[5] Center for Basic Neuroscience Department of Molecular Genetics Howard Hughes Medical Institute University of Texas Southwestern Medical Center Dallas, Texas 75390

[6] Department of Genetics and Molecular Neurobiology Otto von Guericke University Magdeburg D-39106 Magdeburg Germany

[7] Institute of Neurophysiology and Sensory Physiology Heinrich Heine University Düsseldorf D-40225 Düsseldorf Germany

Summary

Synaptogenesis, the generation and maturation of functional synapses between nerve cells, is an essential step in the development of neuronal networks in the brain. It is thought to be triggered by members of the neuroligin family of postsynaptic cell adhesion proteins, which may form transsynaptic contacts with presynaptic α- and β-neurexins and have been implicated in the etiology of autism. We show that deletion mutant mice lacking neuroligin expression die shortly after birth due to respiratory failure. This respiratory failure is a consequence of reduced GABAergic/glycinergic and glutamatergic synaptic transmission and network activity in brainstem centers that control respiration. However, the density of synaptic contacts is not altered in neuroligin-deficient brains and cultured neurons. Our data show that neuroligins are required for proper synapse maturation and brain function, but not for the initial formation of synaptic contacts.

*Correspondence: thomas.sudhof@utsouthwestern.edu (T.C.S.), brose@em.mpg.de (N.B.)

[8] These authors contributed equally to this work.

Introduction

Synapses are asymmetric intercellular contact sites specialized for temporally and spatially precise signal transmission in the brain. They are composed of a presynaptic compartment containing synaptic vesicles clustered around the transmitter release site, or active zone, and a postsynaptic compartment containing the transmitter reception apparatus. During synaptogenesis in human brain development, about 10^{11} nerve cells generate some 10^{15} synapses to establish a complex but precise neuronal network.

Synaptogenesis involves two operationally defined and interdependent cell biological processes that are thought to be mediated by adhesion proteins (Serafini, 1999; Yamagata et al., 2003), the initial contact formation between an axonal growth cone and a target neuron, and the maturation of synaptic contacts through specific assembly and stabilization of pre- and postsynaptic proteins at the contact site. Adhesion proteins involved in the initial formation of synaptic contacts are thought to be encoded by large families of genes and to interact with each other in an isoform-specific manner according to a "lock-and-key" principle in order to allow for the cell-type specificity of synaptogenesis (Sperry, 1963). Adhesion proteins that mediate protein recruitment during synaptogenesis, on the other hand, additionally require specific intracellular binding sites for scaffolding proteins, presynaptic active zone components, and postsynaptic receptors (Garner et al., 2002; Kim and Sheng, 2004; Li and Sheng, 2003; Montgomery et al., 2004; Scheiffele, 2003; Yamagata et al., 2003).

Several recent studies on the molecular mechanism of synaptogenesis indicated a role of neuroligins (NLs) in the formation of synaptic contacts and their maturation (Chih et al., 2005; Chubykin et al., 2005; Dean et al., 2003; Fu et al., 2003; Graf et al., 2004; Levinson et al., 2005; Prange et al., 2004; Scheiffele et al., 2000). NLs are type 1 transmembrane proteins and constitute a family of four (in rodents) or five (in higher primates and humans) postsynaptic cell adhesion proteins that interact with presynaptic α- and β-neurexins (NXs) (Boucard et al., 2005; Ichtchenko et al., 1995; Song et al., 1999; Varoqueaux et al., 2004) via a large extracellular esterase-like domain. Intracellularly, NLs bind to several PDZ domain-containing scaffolding proteins, which in turn interact with postsynaptic transmitter receptors, ion channels, and signaling proteins (Hirao et al., 1998; Irie et al., 1997; Meyer et al., 2004). Similarly, the intracellular domains of NXs, which are also type 1 transmembrane proteins, are indirectly associated with components of the presynaptic transmitter release machinery via interactions with PDZ domain-containing scaffolding proteins (Biederer and Südhof, 2000; Hata et al., 1996).

Expression of NLs in nonneuronal cells induces presynaptic specializations in contacting axons (Scheiffele et al., 2000), and overexpression of NLs in cultured

neurons increases the number of synapses formed (Chih et al., 2005; Dean et al., 2003; Graf et al., 2004; Levinson et al., 2005; Nam and Chen, 2005; Prange et al., 2004), whereas knock-down of NL expression by RNAi leads to a reduction in synapse density (Chih et al., 2005). Analogous effects were observed upon expression of β-NXs in nonneuronal cells (Graf et al., 2004; Nam and Chen, 2005). Overexpression and knock-down of NLs in cultured neurons causes dramatic changes in synaptic activity, which were explained by the dramatic effects of these manipulations on synapse numbers (Chih et al., 2005; Graf et al., 2004). Accordingly, the transsynaptic NL/NX link is thought to be of key importance in the induction phase of synaptogenesis. NLs are thought to trigger synapse formation. In addition, NLs were suggested to also play a role in synapse maturation by recruiting scaffolding proteins, postsynaptic receptors, and signaling proteins to nascent synapses. That NLs are essential for proper brain function is documented by the fact that loss-of-function mutations in the human NL genes *NLGN3* and *NLGN4* cause autism and mental retardation (Chih et al., 2004; Comoletti et al., 2004; Jamain et al., 2003; Laumonnier et al., 2004; Talebizadeh et al., 2006).

To determine the role of NLs in synaptogenesis and synapse function in vivo, we generated and characterized knockout (KO) mice lacking individual or multiple NLs.

Results

Expression of NL Genes in Rodents

The mouse genome contains at least four NL genes: *Nlgn1*, *Nlgn2*, *Nlgn3*, and *Nlgn4* (Ichtchenko et al., 1996; S. Jamain, F.V., N.B, and T. Bourgeron, unpublished data). We employed quantitative Western blotting with isoform-specific antibodies to determine the absolute levels of the four NLs in the brains of newborn and adult mice. In newborn mice, NL 4 is not detectable (Table 1), whereas NLs 1-3 are expressed at moderate levels (NL 1, 65 pg/mg; NL 2, 65 pg/mg; NL 3, 82 pg/mg). In adult mice, only 3% (14 pg/mg) of the total NL protein in brain are contributed by NL 4, while NL 1-3 are expressed at 2- to 3-fold higher levels than in newborn brain (NL 1, 113 pg/mg; NL 2, 170 pg/mg; NL 3, 222 pg/mg). In view of these low levels of NL 4, we focused all subsequent studies on the characteristics of NLs 1-3 in mouse brain.

The mRNAs of NLs 1-3 are expressed at low levels in newborn rat brain and upregulated in parallel (2- to 3-fold) during postnatal development (Figure 1A), reflecting the developmental expression patterns seen for NL protein levels in mouse and rat brain, as described above and in previous studies (Song et al., 1999; Varoqueaux et al., 2004). In situ hybridization experiments showed that in both the newborn and adult rat brain, the mRNAs of NLs 1-3 are coexpressed in almost all neuronal populations (Figures 1B and 1C). Differential expression of NL isoforms is only detectable in the newborn striatum and adult brainstem, hypothalamus, and thalamus, where relative NL 1 mRNA expression levels are lower than those of NL 2 and NL 3 mRNAs (Figures 1B1 and 1C). In agreement with our previous studies on NL mRNA and protein expression (Song et al., 1999; Varoqueaux et al., 2004), areas rich in white matter exhibit only background labeling for NL mRNAs, indicating that oligodendrocytes and fibrous astrocytes express NL mRNAs either at extremely low levels or not at all (Figures 1B and 1C).

Table 1. Expression Levels of Synaptic Proteins in NL 1-3 Triple KO Mice

Presynaptic Proteins		Postsynaptic Proteins	
complexin1	78 ± 4	β-catenin[(a)]	102 ± 3
complexin2	70 ± 2***	N-cadherin	112 ± 3
Munc13-1	106 ± 12	β-dystroglycan	117 ± 15
RIM1/2	95 ± 12	gephyrin	110 ± 11
αSNAP	82 ± 6*	KCC2	80 ± 5**
SNAP-25	88 ± 6	GlyRα	97 ± 3
synaptobrevin 2	77 ± 5*	$GABA_AR\alpha1$	99 ± 1
synaptophysin 1	46 ± 9**	$GABA_AR\beta2/3$	97 ± 4
synaptotagmin 1	78 ± 6*	GluR2/3	83 ± 4
VIAAT[(a)]	76 ± 9	NMDAR1	77 ± 1**
VGluT1	62 ± 4**	NMDAR2A/B	106 ± 9
VGluT2[(a)]	57 ± 2	PSD-95	91 ± 4
calbindin	92 ± 4	neuroligin 4	not detectable

Protein levels in newborn brain homogenates, expressed as percent of wild type levels ± SEM, are listed (wild type, n = 3; TKO, n = 8; [a] control, n = 3; TKO, n = 4; *p < 0.05, **p < 0.01, ***p < 0.001).

Generation of NL KO Mice

To generate mouse KOs lacking NLs 1-3, exon sequences covering the translational start site and at least 380 bp of 5′ coding sequence of the respective genes were deleted by homologous recombination in embryonic stem cells (see Figures S1A and S1B in the Supplemental Data available online). In all cases, this targeting strategy eliminates the respective signal sequences and a significant part of the extracellular esterase-like domain and was therefore predicted to abolish NL expression completely. This was verified by Western blotting of brain homogenates from homozygous KOs using antibodies to the C termini of NLs 1-3, which showed that neither full-length NLs (Figure S1C) nor truncated variants (data not shown) were expressed in the respective KO mice.

KOs lacking individual NLs and all combinations of double KOs were generated by interbreeding and were obtained at the predicted Mendelian frequencies. All single KOs, all types of double heterozygous mice, and triple heterozygous mice were viable and fertile and behaved normally in the cage environment. Likewise, all homozygous double KO combinations were viable. However, they showed drastically reduced reproduction rates and striking deficits in raising their offspring. As a consequence, breeding of triple KOs lacking NLs 1-3 was extremely time consuming, even with very large breeding colonies. Nevertheless, triple KOs were obtained at the predicted Mendelian frequency. They had a slightly reduced body weight as compared to single and double KO littermates (Figure 2A), showed irregular and flat breathing movements as determined by whole-body plethysmography (Figures 2B and 2C), and died within 24 hr after birth. NL 4 levels were not upregulated in triple KO brains (Table 1).

Currently, subcellular localization data on NL proteins in the brain are only available for NL 1 and NL 2. In the

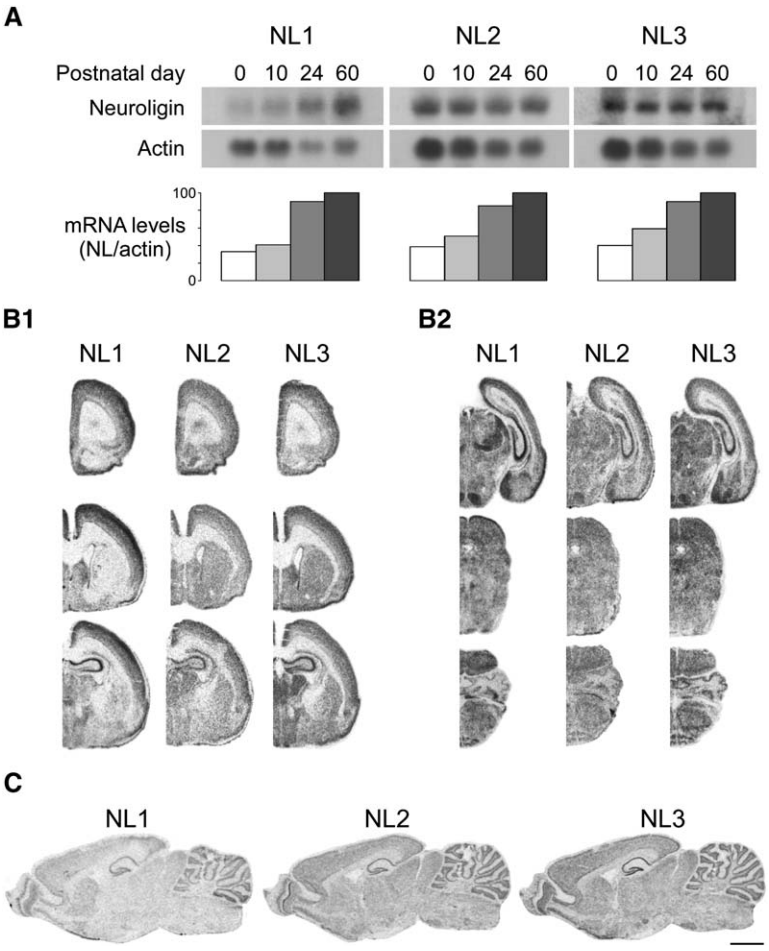

Figure 1. Expression Profiles of NL1, NL2, and NL3 mRNAs during the Synaptogenesis Phase of Rat Brain Development

(A) Northern blot analysis of NL and actin mRNA levels in postnatal brain homogenates at postnatal days 0, 10, 24, and 60. All three NL mRNAs are concomitantly expressed and upregulated during the main synaptogenesis phase of brain development (postnatal days 0–24).

(B1, B2, and C) At all times of postnatal development, NL1, NL2, and NL3 mRNAs are ubiquitously expressed throughout the brain, as shown by in situ hybridization in the newborn (B1 and B2) and the adult rat brain (C). Scale bar, 1.6 mm (B), 3.4 mm (C).

rodent brain, the main NL 1 splice variant is specifically localized to excitatory postsynaptic densities (Song et al., 1999; Chih et al., 2006), whereas the main NL 2 splice variant is specifically localized to inhibitory postsynaptic specializations (Graf et al., 2004; Varoqueaux et al., 2004; Chih et al., 2006). However, both NL 1 and NL 2 alter the density of excitatory and inhibitory synapses when overexpressed in cultured neurons (Graf et al., 2004; Levinson et al., 2005), some less abundant NL 1 and NL 2 splice isoforms are targeted to and induce inhibitory and excitatory synapses, respectively (Chih et al., 2006), and knock-down of individual NLs by RNAi or dominant-negative NLs cause comparable reductions of synapse numbers in neuron cultures (Chih et al., 2005; Nam and Chen, 2005). Moreover, the three NLs present in newborn brain, NL 1-3, are coexpressed in almost all types of neurons (Figure 1B), and only the triple KO lacking NLs 1-3 but none of the single or double KOs showed a perinatally lethal phenotype. As all these findings indicate a significant degree of functional redundancy among NLs 1-3, we studied the phenotype of NL 1-3 triple KOs in more detail.

Brain Cytoarchitecture and Synaptic Protein Expression in NL 1-3 Triple KO Mice

Histological analyses showed that the loss of NL expression in triple KOs had no effect on the gross cytoarchitecture of the newborn brain. The density and layering of neurons in olfactory bulb, cortex, and hippocampus of triple KOs were indistinguishable from those in triple heterozygous controls (Figure S2). Even brain regions that are mature at birth, such as the brainstem, did not show evidence of cell loss (data not shown).

Analysis of total brain expression levels of selected synaptic marker proteins in triple KOs and wild-type controls by quantitative Western blotting revealed a complex pattern of changes (Table 1). The levels of all tested general, excitatory, and inhibitory synaptic vesicle markers were reduced in triple KO brains. Likewise, the levels of the soluble SNARE regulators complexin 2 and αSNAP were significantly lower in triple KOs as compared to controls, whereas the expression levels of the active zone proteins Munc13-1 and RIM1/2, the SNARE SNAP-25, and calbindin were unchanged. The Cl^- channel KCC2 showed reduced expression levels in triple KO brains, while the expression of gephyrin, β-dystroglycan, $GABA_A$ receptor subunits α1 and β2/3, and glycine receptor α subunits, all markers for GABAergic/glycinergic postsynapses, was normal. Upon analysis of markers of glutamatergic excitatory postsynapses, only the expression levels of NMDAR1 were found to be reduced significantly in triple KOs. The levels of PSD-95 and of the glutamate receptor subunits GluR2/3 and NMDAR2A/B were similar in triple KO and control brains. The finding that the levels of integral components of synaptic contacts, such as the active zone markers Munc13-1 and

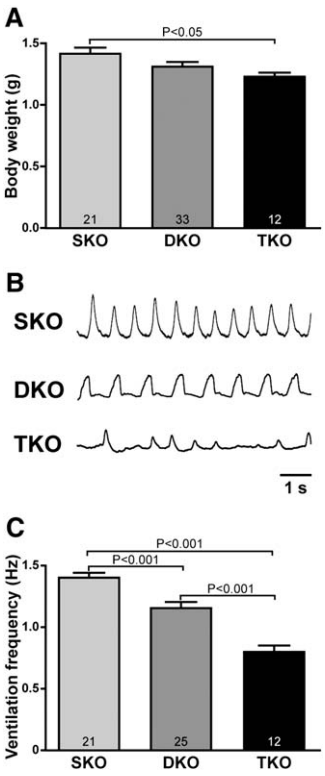

Figure 2. Essential Role of NLs in Respiratory Function

(A) Averaged body weight of NL single (SKO), double (DKO), and triple (TKO) KO mice. (B) Representative ventilation traces and (C) averaged ventilation frequencies of different NL mutant mice as measured by whole-body plethysmography. Numbers within the bar graphs indicate the number of mice tested for each genotype. Error bars indicate SEM.

RIM1/2, are not affected in the NL 1-3 triple KO whereas the expression levels of vesicle markers are reduced is compatible with the notion that loss of NLs results in aberrant recruitment of synaptic proteins or vesicles but does not cause changes in the number of synaptic contacts (see below).

Synapse Formation and Function in Cultured NL 1-3 Triple KO Neurons

One of the best characterized NL interaction partners is the postsynaptic density protein PSD-95. It binds to NLs via its third PDZ domain (Irie et al., 1997), as well as to K^+ channels (Kim et al., 1995), NMDA receptor subunits (Kornau et al., 1995), and other scaffolding and signaling proteins at its two other PDZ domains and additional binding sites (Garner et al., 2002; Li and Sheng, 2003; Montgomery et al., 2004; Scheiffele, 2003). PSD-95 also binds to stargazin, which in turn interacts with AMPA receptors (Fukata et al., 2005; Schnell et al., 2002). Thus, PSD-95 represents an adaptor between synaptic cell adhesion and the postsynaptic signaling apparatus. Experiments in neuron cultures showed that PSD-95, presumably through its interaction with NLs, and stargazin mediate the synaptic recruitment of glutamate receptors (El-Husseini et al., 2002; Fukata et al., 2005; Levinson et al., 2005; Prange et al., 2004; Schnell et al., 2002).

To examine the role of NLs in synaptogenesis and the regulation of the glutamate receptor complement at synapses, we studied glutamatergic synaptic transmission in cocultures of neocortical explants and dissociated neocortical target neurons from the same NL 1-3 triple KO mice by whole-cell patch-clamp recording at 13–15 DIV (Mohrmann et al., 1999). Cultures from triple heterozygous littermates served as controls and yielded data that were very similar to those obtained in preparations from an unrelated wild-type mouse strain (Figures S3C–S3E). In this system, the frequency and amplitude of miniature excitatory postsynaptic currents (mEPSCs), the AMPA and NMDA receptor-mediated contributions to evoked excitatory postsynaptic currents (eEPSCs), and the specific loss of AMPA or NMDA receptors from postsynapses can be measured with high fidelity (Mohrmann et al., 1999) and can serve as readouts for the effects of NL deletion on synaptogenesis and synaptic receptor recruitment. Neither the frequency nor the amplitude of AMPA mEPSCs differed significantly between neurons obtained from triple KOs and heterozygous controls (Figures S3A, S3C, and S3D). These results are in line with recent electrophysiological data obtained in RNAi knock-down experiments on cultured neurons, where a strong reduction of NL 1-3 expression had little effect on AMPA mEPSC frequency or amplitude (Chih et al., 2005). In subsequent experiments, we examined the ratio of evoked NMDA receptor- and AMPA receptor-mediated eEPSCs at the same set of synapses. No significant differences in AMPA eEPSCs, NMDA eEPSCs, or their ratio were found between triple KO neurons and heterozygous control neurons in this culture preparation (Figures S3B and S3E). In contrast, NMDA receptor-mediated, but not AMPA receptor-mediated, synaptic transmission onto CA1 pyramidal cells appears to be perturbed in acute hippocampal slices from NL 1 KO animals (A.A. Chubykin, J.R. Gibson, D. Atasoy, N.B., E.T. Kavalali, and T.C.S, unpublished data).

The electrophysiological features of NL 1-3 triple KO cortical neurons agreed with the morphological characteristics of hippocampal and cortical neurons from these mutants. Immunofluorescence double staining of the synaptic markers synapsin and PSD-95 revealed no differences in synapse densities of neuron cultures from triple KO and control hippocampus (Figures 3A and 3B). Moreover, the ultrastructure of synapses formed by NL 1-3 triple KO neurons was indistinguishable from the triple heterozygous control situation, as assessed by morphometric electron microscopic analyses of cortical explants at DIV 18 (Figures 3C and 3D). These electrophysiological and morphological findings indicate that the initial formation of synaptic contacts does not depend on NLs.

Respiratory Failure in NL 1-3 Triple KO Mice

Because of the apparent synaptogenic effects of NL overexpression in cultured neurons (Chih et al., 2005; Dean et al., 2003; Graf et al., 2004; Levinson et al., 2005; Nam and Chen, 2005; Prange et al., 2004; Scheiffele et al., 2000) and the proposed role of NLs in the synaptic recruitment of glutamate receptors (Chih et al., 2005; Dean et al., 2003; Graf et al., 2004; Levinson et al., 2005; Nam and Chen, 2005; Prange et al., 2004; Scheiffele et al., 2000; Serafini, 1999) we had initially predicted that KO of all NLs in mouse brain neurons would

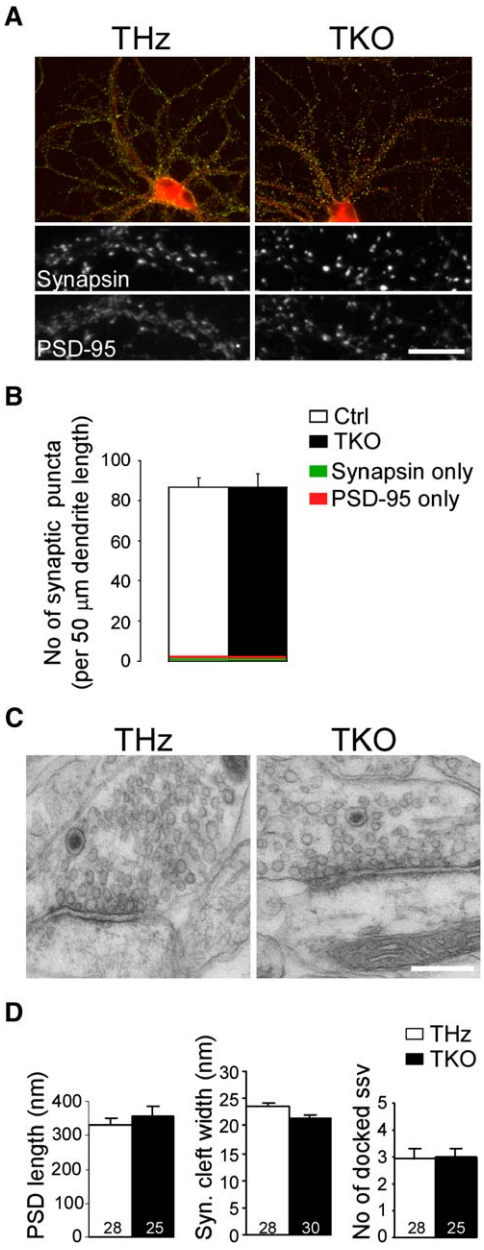

Figure 3. Normal Synaptogenesis and Synaptic Morphology in NL 1-3 Triple KO Hippocampal and Neocortical Neurons

(A) Combined immunofluorescence detection of synapsin (presynaptic marker) and PSD-95 (glutamatergic postsynaptic marker) in cultured hippocampal neurons, showing that synapses are formed at normal densities by the NL 1-3 triple KO (TKO) neurons, as compared to triple heterozygous controls (THz).

(B) Quantification of synapsin-labeled puncta per dendrite length of control (ctrl) and NL1-3 triple KO (TKO) neurons. The vast majority (>98%) of these puncta were found in close apposition to PSD-95 immunoreactive puncta.

(C and D) Cortical explants after 2 weeks in culture. Mature synaptic specializations (C) were observed on NL triple KO (TKO) as well as on control (THz) neurons, and synaptic parameters (length of the postsynaptic density [PSD], width of the synaptic cleft, number of docked vesicles) were similar in both experimental groups (D).

Numbers within the bar graphs indicate the number of synapses studied. Scale bars, 20 μm (A), 150 nm (C). Error bars indicate SEM.

result in decreased synapse numbers and/or aberrant glutamatergic synaptic transmission, but our experimental approaches to test these predictions in cultured neurons failed to uncover phenotypic changes in NL triple KO neurons (Figures 3 and S3). A reason for this finding may be that phenotypic changes induced by NL deletion can be obscured in neuron culture preparations.

We therefore turned to the most obvious phenotypic characteristic of the triple KOs, their early postnatal death, which is most likely caused by respiratory failure, as NL 1-3 triple KOs show flat and irregular breathing movements (Figure 2). We examined the function of the brainstem respiratory network consisting of the pre-Bötzinger complex (PBC) and the hypoglossal nucleus (NH) in acute brainstem slices from triple KO mice by whole-cell patch-clamp recordings (Missler et al., 2003; Zhang et al., 2005). Because this type of analysis required large numbers of triple KO animals and it is practically impossible to obtain sufficient numbers of NL 1-3 triple KOs and wild-type control littermates, we followed a breeding strategy using mice that were homozygous KOs for one NL allele (mostly NL 3, some NL 1, no NL 2) and heterozygous for the two others. As a consequence, single KO (NL 3 or NL 1, no NL 2) and double KO littermates (NL 1 and NL 3) had to serve as controls in these experiments. For statistical purposes, the datasets from these two control groups of animals were pooled separately and are referred to as single KO and double KO below. In all cases, the pooled data from single KOs approached wild-type control levels, which were measured in a wild-type line with a similar mosaic genetic background as the NL 1-3 triple KO (data not shown). Essentially, this statistical analysis underestimates phenotypic changes contributed by the KO of NL 1 or NL 3.

We first recorded voltage-activated Na^+, K^+, and Ca^{2+} currents in the PBC, which is essential for generating a normal respiratory rhythm. Neither Na^+ nor K^+ or Ca^{2+} current densities were significantly altered in NL 1-3 triple KO neurons of the PBC (Figure S4). To test whether synaptic function is impaired in the brainstem of triple KOs, we next analyzed synaptic transmission in the PBC. Spontaneous postsynaptic currents (sPSCs) measured in whole-cell patch-clamp recordings from PBC neurons revealed a dramatically reduced frequency of total sPSCs as well as of pharmacologically separated GABAergic and glycinergic sPSCs in NL 1-3 triple KOs as compared to single KOs, while sPSC amplitudes were less affected (Figures 4A–4F). Different double KO combinations caused a similar but less pronounced phenotype. Analysis of the amplitude distribution of GABAergic and glycinergic sPSCs showed two distinct populations in single KOs with mean amplitudes of 35 and 100 pA, which most likely correspond to miniature and action potential driven events, respectively (Figure 4F). Deletion of two NLs decreased the high-amplitude population of GABAergic and glycinergic sPSCs by more than 50%, while the number of sPSCs with lower amplitude was only moderately changed (<20%). In triple KOs, the number of GABAergic and glycinergic sPSCs with lower and higher amplitude were decreased by 85% and 95%, respectively. In an additional series of experiments, we analyzed miniature

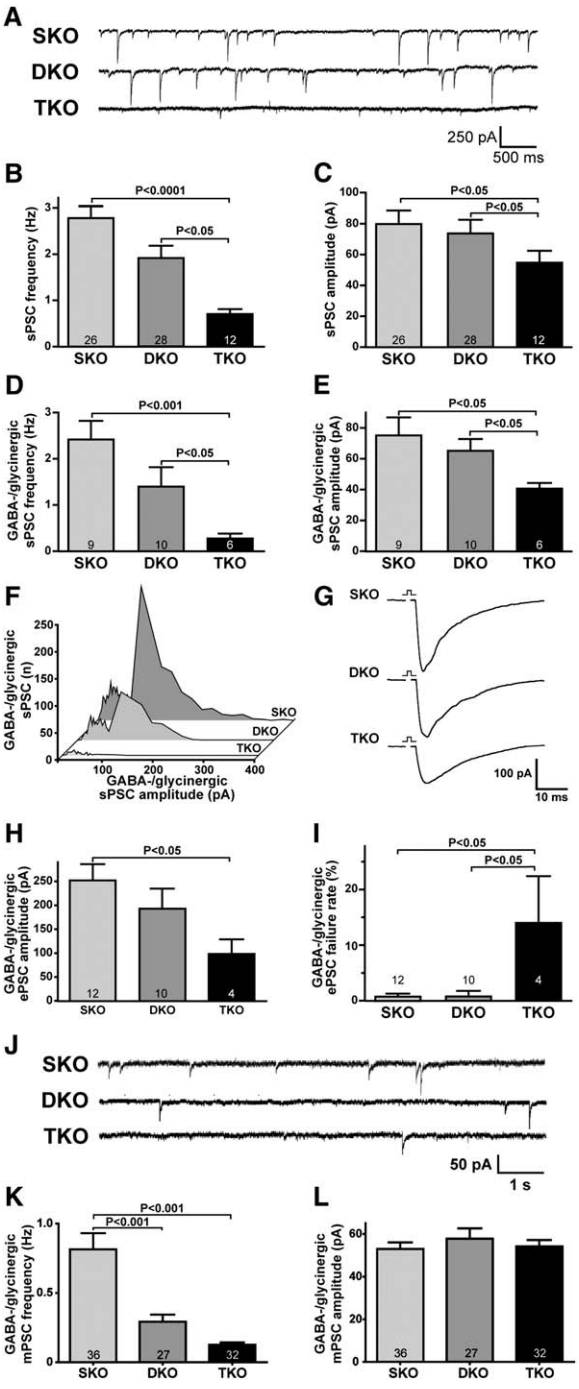

Figure 4. Impaired GABAergic/Glycinergic Neurotransmission in the Respiratory Centers of the NL 1-3 Triple KO

(A) Representative recordings of pharmacologically isolated spontaneous GABAergic/glycinergic postsynaptic currents (sPSC) in brainstem PBC neurons. Slices were prepared from littermate NL single (SKO), double (DKO), and triple KO (TKO) mice.

(B and C) Frequency (B) and amplitude (C) of total sPSCs in PBC neurons.

(D–F) Frequency (D), amplitude (E), and amplitude distribution (F) of pharmacologically isolated GABAergic/glycinergic sPSCs in PBC neurons.

(G and H) Impaired evoked GABAergic/glycinergic neurotransmission in hypoglossal neurons from NL KO mice. Sample traces of evoked GABAergic/glycinergic ePSCs (G) and the mean amplitudes of evoked GABAergic/glycinergic ePSCs in response to extracellular stimuli (H) are given.

GABAergic and glycinergic PSCs (mPSCs) in PBC neurons directly. While the frequency of GABAergic/glycinergic mPSCs was reduced by 80% in triple KO cells as compared to single KO control cells, the amplitudes of GABAergic/glycinergic mPSCs were similar in all tested genotypes (Figures 4J–4L).

To examine the effects of the NL 1-3 deletion on glutamatergic synaptic transmission in the respiratory brainstem, we monitored pharmacologically isolated spontaneous glutamatergic postsynaptic currents in PBC neurons. In comparison to data from single KO slices, the frequency of glutamatergic sPSCs in PBC neurons was decreased in NL 1-3 triple KO slices (Figures 5A and 5B). The amplitudes of glutamatergic sPSCs were similar in all tested genotypes (Figures 5C and 5E). In order to detect differential effects of the NL 1-3 triple KO on glutamatergic and GABAergic/glycinergic synaptic transmission, we determined the relative contribution of glutamatergic sPSCs and GABAergic/glycinergic sPSCs to the total synaptic events in a subset of experiments. In all single KOs, most events were GABAergic/glycinergic sPSCs (80%), and glutamatergic sPSCs contributed only 20% of the total synaptic activity (Figure 5D). This ratio is very similar to that observed in respiratory brainstem slices from newborn wild-type mice (Missler et al., 2003). Deletion of two or three NLs dramatically changed the balance between glutamatergic and GABAergic/glycinergic sPSCs, with glutamatergic sPSCs contributing 70% and GABAergic/glycinergic sPSCs contributing 30% of all synaptic events in NL 1-3 triple KOs (Figure 5D). This change did not result from an increase of total glutamatergic activity, but was rather a consequence of the strong decrease in GABAergic/glycinergic sPSC frequency. When we analyzed miniature glutamatergic mPSCs in PBC neurons directly, we observed an 80% reduction in mPSC frequency in triple KO cells as compared to single KO controls, whereas the amplitudes of glutamatergic mPSCs were similar in all tested genotypes (Figures 5H–5J).

Finally, we examined electrically evoked synaptic transmission in the NH. For this purpose, we stimulated neurons in the vicinity of the PBC and measured synaptic transmission to NH neurons by whole-cell patch-clamp recordings in the presence of CNQX for GABAergic/glycinergic ePSCs, or bicuculline/strychnine for the analysis of glutamatergic ePSCs. Compared to slices from single KOs, the average amplitude of GABAergic/glycinergic ePSCs was strongly decreased in NH neurons from NL 1-3 triple KOs, whereas GABAergic/glycinergic ePSC amplitudes in double KO neurons were not changed significantly (Figures 4G and 4H). Despite the fact that we used supramaximal stimulation, the failure rate of GABAergic/glycinergic ePSCs was strongly increased in NL 1-3 triple KO neurons as compared to controls (Figure 4I). In contrast to GABAergic/glycinergic

(I) Failure rates of evoked GABAergic/glycinergic neurotransmission in hypoglossal neurons from NL KO mice.

(J) Representative recordings of pharmacologically isolated spontaneous miniature GABAergic/glycinergic mPSCs in PBC neurons.

(K and L) Frequency (K) and amplitude (L) of GABAergic/glycinergic mPSCs in PBC neurons.

Numbers within or above the bar graphs indicate the number of mice tested for each genotype. Error bars indicate SEM.

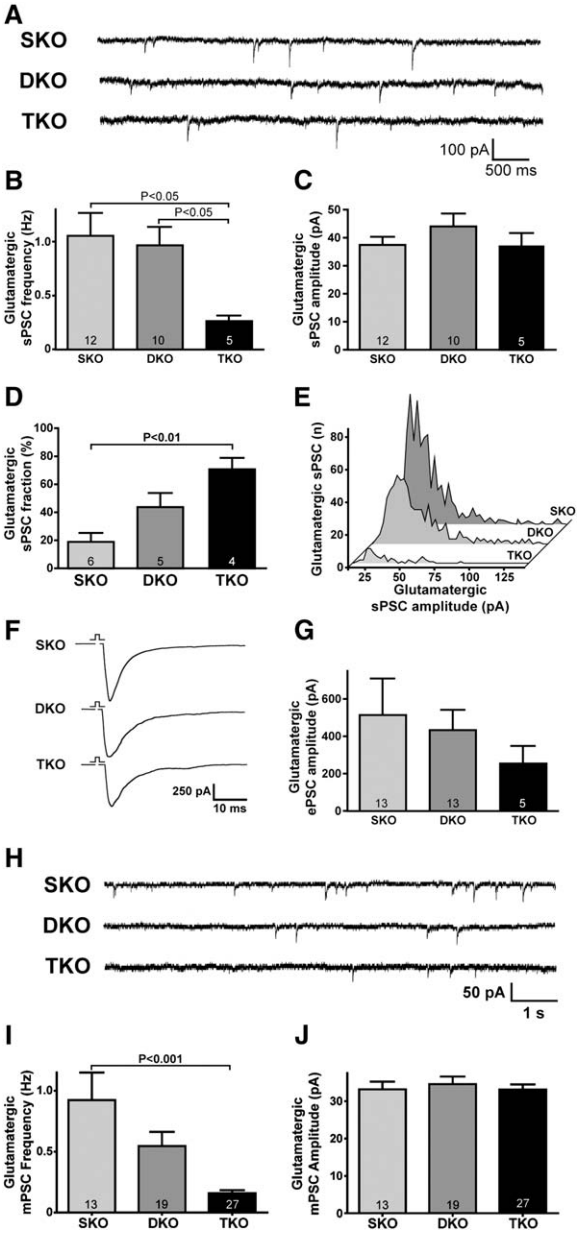

Figure 5. Impaired Glutamatergic Neurotransmission in the Respiratory Centers of the NL 1-3 Triple KO

(A) Representative recordings of pharmacologically isolated spontaneous glutamatergic postsynaptic currents (sPSC) in brainstem PBC neurons. Slices were prepared from littermate NL single (SKO), double (DKO), and triple KO (TKO) mice.

(B and C) Frequency (B) and amplitude (C) of glutamatergic sPSCs in PBC neurons.

(D) CNQX-sensitive glutamatergic fraction of sPSCs, expressed as percent of total sPSCs in PBC neurons of NL KO mice.

(E) Amplitude distribution of spontaneous glutamatergic sPSCs in PBC neurons of NL KO mice.

(F and G) Reduced evoked excitatory neurotransmission in hypoglossal neurons from NL KO mice. Sample traces of evoked glutamatergic ePSCs (F) and the mean amplitudes of evoked glutamatergic ePSCs in response to extracellular stimuli (G) are given.

(H) Representative recordings of pharmacologically isolated spontaneous glutamatergic mPSCs in PBC neurons.

(I and J) Frequency (I) and amplitude (J) of glutamatergic mPSCs in PBC neurons.

Numbers within the bar graphs indicate the number of mice tested for each genotype. Error bars indicate SEM.

ePSCs, the amplitudes of glutamatergic ePSCs were not significantly different in NH neurons from single, double, or triple KOs (Figures 5F and 5G), and failure rates were similar in all tested genotypes (3.9% ± 2.3%, n = 13, 5.0% ± 3.5%, n = 13, and 4.0% ± 1.2%, n = 5, for single, double, and triple KOs, respectively).

Synaptogenesis in the Brainstem of NL 1-3 Triple KO Mice

The neuronal network of the respiratory brainstem in mice is almost mature at the time of birth, with most synaptic contacts already established. It can therefore serve as an ideal system for the analysis of the consequences of NL deletion on synaptogenesis in the intact brain of newborn NL 1-3 triple KOs.

To examine whether the striking functional deficits in the respiratory brainstem of NL 1-3 triple KOs reflect aberrant synaptogenesis, we performed a detailed morphometric analysis of synapse types and densities at the light microscopic and ultrastructural level. Immunofluorescence staining of brainstem sections for the presynaptic marker synaptophysin 1 showed no differences in the overall density of presynaptic terminals in the PBC, the NH, and the neighboring inferior olive when images from control and NL 1-3 triple KO mice were compared. However, the ratio between the number of glutamatergic terminals as assessed by VGluT1/2 immunoreactivity and the number of GABAergic/glycinergic terminals as assessed by VIAAT immunoreactivity was slightly increased in the PBC and inferior olive, but not in the NH of triple KOs (Figures 6A and 6B). This change was due to a very subtle alteration in the absolute numbers of glutamatergic and GABAergic/glycinergic synapses, which was not statistically significant and became only apparent when the ratios between the numbers of the two types of synapses were analyzed.

Using immunofluorescence staining for inhibitory postsynaptic markers in the PBC, we found a 30% reduction in the number of postsynaptic clusters containing $GABA_AR\alpha1$ but no significant changes in the number of postsynaptic clusters containing gephyrin or $GlyR\alpha$ subunits (Figures 6C and 6D). Moreover, the staining intensity of individual $GABA_AR\alpha1$ clusters appeared to be reduced in triple KO preparations (Figure 6C). Ultrastructural analysis of the PBC revealed synaptic specializations whose numbers were similar in NL 1-3 triple KO and control samples (Figures 6E and 6F).

In a final series of experiments, we performed double labeling experiments in order to determine the number of matched and mismatched pre- and postsynaptic glutamatergic (staining for VGluT1/VGluT2 and PSD-95) and GABAergic/glycinergic compartments (staining for VIAAT and gephyrin) in control and NL 1-3 triple KO PBC (Figure 7). We had to use an alternative fixation method for these double staining experiments, i.e., formaldehyde instead of methanol (see Experimental Procedures). As a consequence, the datasets of the single (Figures 6A–6D) and double staining experiments (Figure 7) are not directly comparable. In the case of both, glutamatergic and GABAergic/glycinergic structures, the number of "orphan" pre- or postsynaptic structures was high in the newborn PBC but very similar in control and triple KO. Likewise, the number of pre- and postsynaptically double labeled glutamatergic and

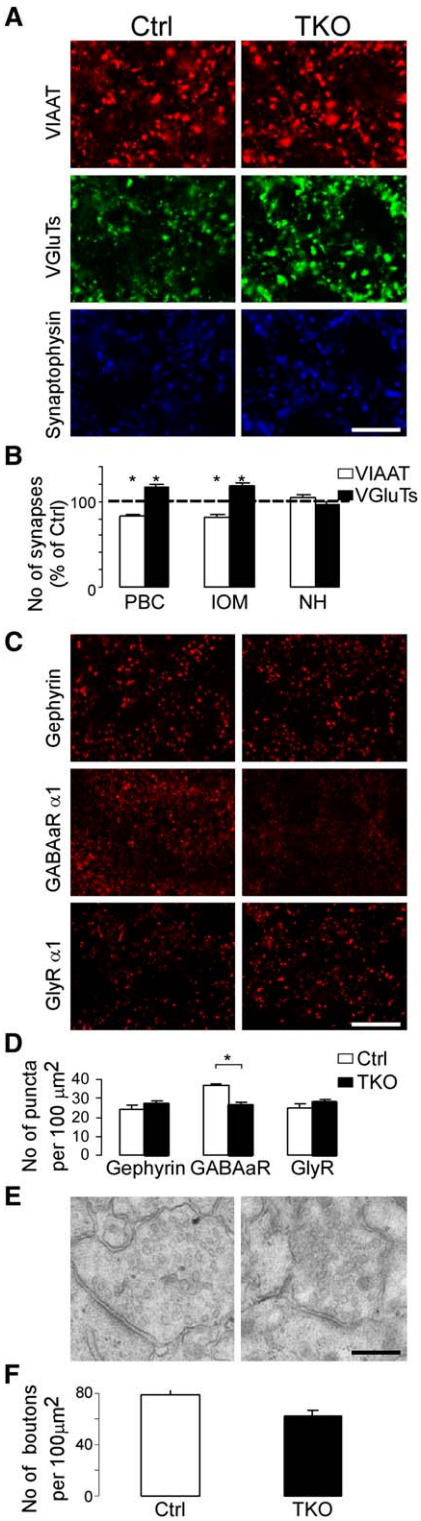

Figure 6. Altered Ratio of Glutamatergic versus GABAergic/Glycinergic Terminals but Normal Overall Synapse Numbers in the Respiratory Centers of the NL 1-3 Triple KO

(A) Representative micrographs of the PBC area of control (Ctrl) and NL 1-3 triple KO (TKO) sections after triple labeling for GABAergic/glycinergic (stained for VIAAT, red), glutamatergic (stained for VGluT1/2, green), and all presynapses (stained for synaptophysin 1, blue).

(B) Number of GABAergic/glycinergic (white) and glutamatergic (black) synapses in the PBC, inferior olive (IOM), and hypoglossal nucleus (NH) of NL 1-3 triple KOs plotted as the percentages of glutamatergic and GABAergic/glycinergic synapses observed in the control (Ctrl) (*$p < 0,001$). The total number of synapses was not significantly different in the two experimental groups.

(C) Representative micrographs of the PBC area of control (Ctrl) and NL 1-3 triple KO (TKO) sections after labeling for gephyrin, $GABA_AR\alpha1$, and $GlyR\alpha1$.

(D) Quantification of immunoreactive puncta (*$p < 0.001$).

(E and F) Ultrastructural analysis of the PBC showing synaptic specializations in NL 1-3 triple KO (TKO) and control (Ctrl) preparations.

(F) Quantification of synapse numbers as identified by ultrastructural analysis.

Scale bars, 10 μm (A and C), 250 nm (E). Error bars indicate SEM.

GABAergic/glycinergic synapses was almost identical in control and triple KO PBC. Together with our morphological data on cortical explants and cultured hippocampal neurons from NL 1-3 triple KO brains (Figure 3), these findings indicate that NLs do not control the initial formation of synaptic contacts in the brain as synapse numbers remain unchanged in the absence of NLs. Consequently, the reduced expression levels of synaptic vesicle markers in NL 1-3 triple KO brains (Table 1) are unlikely to be due to prominent changes in synapse numbers, but may rather reflect aberrant protein equipment of synaptic vesicles or changes in total vesicle numbers.

Discussion

The present data show that NLs are essential for proper synapse and brain function but not for the formation of synaptic contacts per se. Loss of NLs results in a dramatic decrease in spontaneous GABAergic/glycinergic activity (Figure 4) and moderately reduced spontaneous glutamatergic activity (Figure 5) in the respiratory brainstem, which causes respiratory failure (Figure 2). The altered GABAergic/glycinergic activity in the respiratory brainstem of triple NL 1-3 KOs appears to be partly due to altered postsynaptic recruitment of $GABA_A$ receptors (Figures 6C and 6D), but a presynaptic dysfunction may also contribute (Table 1). Similarly, a combination of post- and presynaptic perturbations likely underlies the glutamatergic dysfunction in NL 1-3 triple KO brainstem. Interestingly, NLs influence the balance between glutamatergic and GABAergic/glycinergic transmission in the respiratory brainstem without affecting the total number of synapses (Figures 4–7). Triple NL 1-3 KOs exhibit an increased ratio of glutamatergic versus GABAergic/glycinergic synapses (Figures 6A–6D) and an increase in the ratio of spontaneous glutamatergic versus GABAergic/glycinergic synaptic activity (Figure 5D) in the respiratory rhythm generating brainstem network.

Synaptogenesis and Synaptic Function in NL 1-3 Triple KO Mice

None of our analyses on NL 1-3 triple KOs yielded data that would indicate a significant role of NLs in the initial formation of synaptic contacts in vivo. Irrespective of the preparation or brain region tested, synapse numbers were not affected by NL loss (Figures 3A, 3B, 6, and 7). Even the change in the ratio between the number of glutamatergic synapses and GABAergic/glycinergic synapses that we observed in the brainstem of NL 1-3 triple KOs (Figures 6A and 6B) was caused by only very

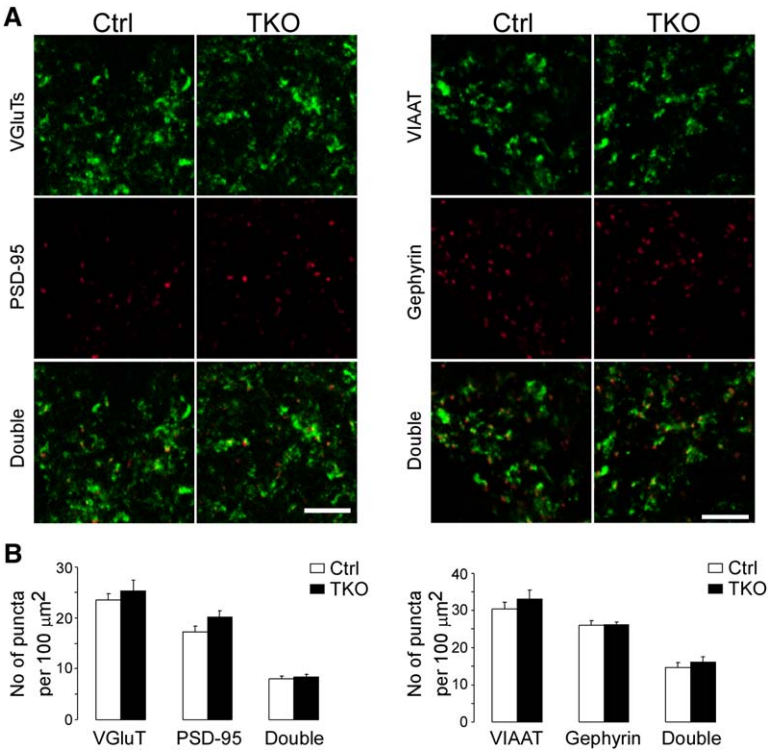

Figure 7. Properly Aligned Pre- and Postsynaptic Specializations in the Respiratory Centers of the NL 1-3 Triple KO

(A) The left panel shows representative micrographs of the PBC area of control (Ctrl, n = 4) and NL 1-3 triple KO (TKO, n = 2) sections after double labeling for glutamatergic presynapses (stained for VGluT1/2, green) and excitatory postsynapses (stained for PSD-95, red). The right panel shows representative micrographs of the PBC area of control (Ctrl, n = 5) and NL 1-3 triple KO (TKO, n = 4) sections after double labeling for GABAergic/glycinergic presynapses (stained for VIAAT, green) and inhibitory postsynapses (stained for gephyrin, red).

(B) The left panel shows the quantification of isolated and colocalized VGluT1/2 and PSD-95 puncta in the PBC of control (Ctrl, white) and NL 1-3 triple KO mice (TKO, black). The right panel shows the quantification of isolated and colocalized VIAAT and gephyrin puncta in the PBC of control (Ctrl, white) and NL 1-3 triple KO mice (TKO, black).

The total number of synapses was not significantly different in the two experimental groups. Scale bars, 30 μm. Error bars indicate SEM.

subtle and statistically insignificant changes in absolute GABAergic/glycinergic (decrease) and glutamatergic synapse numbers (increase) in the range of 15%, without affecting the total synapse number. These findings are not entirely congruent with the effects of NL knockdown in cultured neurons (Chih et al., 2005) and indicate that NLs determine functional parameters of synapses by regulating the recruitment of synaptic proteins (e.g., $GABA_A$ receptors; Figures 6C and 6D) or organelles (e.g., synaptic vesicles; Table 1), rather than the generation of synapses per se.

At first glance, our electrophysiological studies in brainstem seem to indicate that deletion of NLs 1-3 affects inhibitory synaptic transmission more strongly than excitatory transmission. However, as mentioned above, the necessity to produce large numbers of NL 1-3 triple KOs forced us to use single NL 1 and NL 3 KOs as well as NL 1/3 double KOs as littermate controls in our electrophysiological analyses (but note that for electron microscopic [Figures 6E and 6F] and Western blot studies [Table 1], wt mice with a similar mosaic genetic background were used as controls, and for light microscopic studies [Figures 3A, 3B, 6A–6D, and 7], mostly triple heterozygous littermate controls were used; see Experimental Procedures). Given that the main splice isoforms of both NL 1 (Song et al., 1999; Chih et al., 2006) and NL 3 (F.V. and S. Jamain, unpublished data) are preferentially localized to glutamatergic synapses, our approach is therefore likely to result in an underestimation of phenotypic changes in glutamatergic synapses of NL 1-3 triple KOs. A biological reason for a preferential effect of the NL 1-3 triple KO on GABAergic/glycinergic synapses may be the fact that glutamatergic synapses, in contrast to GABAergic/glycinergic synapses, contain multiple transsynaptic cell adhesion and signaling systems that interact with intracellular scaffolding proteins (Garner et al., 2002; Kim and Sheng, 2004; Li and Sheng, 2003; Montgomery et al., 2004; Scheiffele, 2003; Yamagata et al., 2003). These may act in parallel with the NL/NX system and may therefore be able to partially mask the effects of NL loss. This type of compensation is likely to be much less efficient in GABAergic/glycinergic synapses.

Nevertheless, our analysis of glutamatergic transmission did reveal significant functional changes in NL 1-3 triple KOs. Most notably, the frequency of glutamatergic sPSCs in the PBC of NL 1-3 triple KOs was reduced, while ePSC amplitudes were similar in all NL KO combinations (Figures 5A–5C), and the number of glutamatergic synapses was unaltered in the brainstem of NL 1-3 triple KOs (Figures 6A, 6B, and 7). Evoked glutamatergic ePSC amplitudes in NH were slightly reduced in NL 1-3 triple KOs (Figures 5F and 5G), but cultured cortical neurons from NL 1-3 triple KOs showed no evidence of changes in glutamatergic transmisssion (Figure S3). Interestingly, our analysis of miniature glutamatergic mPSCs revealed a strongly reduced mPSC frequency but normal mPSC amplitudes in the PBC of NL 1-3 triple KOs (Figures 5H–5J). These findings, together with all other data on brainstem morphology and glutamatergic transmission, indicate that the absence of NLs 1-3 leads to the functional shut-down of a significant number of glutamatergic synapses, hence the strong reduction in sPSC and mPSC frequency (Figures 5B and 5I) with no change in sPSC and mPSC amplitudes (Figures 5C and 5J) or synapse numbers (Figures 6 and 7). This shut-down of synapses may not only be caused by postsynaptic changes but may also be due to a presynaptic dysfunction, a notion that is supported by the finding that expression levels

of synaptic vesicle proteins are reduced in NL 1-3 triple KO brains (Table 1).

Spontaneous GABAergic/glycinergic sPSC amplitudes in the PBC and evoked GABAergic/glycinergic ePSC amplitudes in NH were both strongly reduced in NL 1-3 triple KOs (Figures 4E and 4H). Together with the observation that the number of postsynaptic clusters containing $GABA_AR\alpha1$ were reduced while the number of postsynaptic clusters containing gephyrin or $GlyR\alpha$ subunits (Figures 6C and 6D) and the numbers of inhibitory synapses as determined by double labeling for VIAAT and gephyrin (Figure 7) were unaltered in the brainstem of NL 1-3 KOs, these data indicate that GABAergic synaptic contacts are formed initially but do not function properly in the absence of NLs, possibly due to a deficiency in the recruitment of receptors to GABAergic synapses. As seen with glutamatergic synapses, GABAergic/glycinergic mPSC frequencies are reduced but mPSC amplitudes are unaltered in NL 1-3 triple KO PBC (Figures 4J–4L). This observation likely reflects a functional shut-down of a subpopulation of GABAergic synapses due to the loss of postsynaptic receptors (Figures 6C and 6D) and/or a presynaptic dysfunction, such as a partial loss of synaptic vesicles or their aberrant equipment with proteins (Table 1).

The dramatic decrease in overall spontaneous synaptic activity in the respiratory brainstem of NL 1-3 triple KOs (Figures 4A, 4B, 5A, and 5B) is likely to be caused by the combined glutamatergic and GABAergic synaptic dysfunction. GABAergic and glycinergic transmission in the newborn respiratory brainstem is still largely excitatory (Ritter and Zhang, 2000). Consequently, a combined reduction in glutamatergic and GABAergic synaptic transmission will result in reduced excitatory drive and low overall spontaneous synaptic activity. Changes in neuronal excitability do not appear to contribute to the decreased network activity in NL 1-3 triple KOs, as neuronal Na^+, K^+, and Ca^{2+} currents were normal in these mice (Figure S4). Given that NLs do not regulate initial synaptogenesis per se, the increase in glutamatergic versus GABAergic/glycinergic synapse ratios observed in the PBC and inferior olive in NL 1-3 triple KOs may be partly due to homeostatic adaptations that occur as a consequence of the strongly reduced network activity.

Redundancy among NLs

At first glance, the fact that all single NL KOs as well as all combinations of NL double KOs are viable whereas NL 1-3 triple KOs die shortly after birth may indicate a significant degree of functional redundancy among NLs 1-3, which even extends to the differentially localized dominant splice isoforms of NL 1 and NL 2. However, an analysis of NL 2 distribution in NL 1 single KO neurons showed that the main NL 2 splice variant is not recruited to glutamatergic synapses when NL 1 is absent (F.V., and N.B., unpublished data), demonstrating that these NLs do not simply replace each other ectopically if one of them is eliminated. In view of these findings, we propose that the perinatal lethality of the NL 1-3 triple KOs is due to a synthetic lethal effect of the combination of the three NL single KOs, where subtle mutant synaptic phenotypes accumulate to cause the failure of essential brain networks, such as the respiratory system, and death.

NL KO Mice versus NL Knock-Down and Overexpression in Cultured Neurons

The present study shows that NLs are dispensable for the initial formation of synapses in cultured neurons (Figure 3) and in the intact brain (Figures 6 and 7). This finding is in agreement with data obtained in α-NX KOs, where loss of all three α-NXs has very little effect on overall synapse densities (Missler et al., 2003) but, as mentioned above, does not entirely agree with results obtained in experiments involving NL overexpression or RNAi knock-down of NLs in cultured neurons (Dean et al., 2003; Graf et al., 2004; Chih et al., 2005; Levinson et al., 2005; Nam and Chen, 2005; Prange et al., 2004; Scheiffele et al., 2000). To a certain degree, the discrepancy between the present data on NL 1-3 triple KOs and the data obtained in NL overexpression experiments can be formally dismissed because the overexpression data document that NLs are *sufficient* to trigger synaptogenesis in vitro whereas our present KO study documents that they are *not necessary* for this process in vivo. However, even in view of these considerations, certain aspects of the discrepancy between the present data on NL 1-3 triple KOs and the data obtained after RNAi knock-down of NLs in cultured neurons remain. For example, even the knock-down of a single NL causes strong reductions in synapse numbers of cultured neurons in vitro (Chih et al., 2005) whereas KO of all NL expression has no effect on synapse numbers in cultured neurons in vitro (Figure 3) or in the intact brain in vivo (Figures 6 and 7).

We propose that one explanation for this discrepancy may be an indirect and activity-dependent homeostatic effect rather than a direct effect of NL RNAi knock-down on synaptogenesis in cultured neurons. Such activity-dependent homeostatic regulation of synapse densities has been described in numerous studies (Turrigiano and Nelson, 2004) and occurs even when activity changes are very small. For example, synaptophysin 1-deficient neurons, which show no electrophysiologically measurable functional deficit (McMahon et al., 1996), generate fewer synapses than wild-type neurons in coculture (Tarsa and Goda, 2002), indicating that even subtle functional differences between neurons cause a competition situation, where functionally disadvantaged neurons maintain their synapses less efficiently. A similar situation may arise in the published cell culture experiments involving RNAi knock-down of NLs (Chih et al., 2005), where knock-down after plasmid transfection results in a mixed population of transfected and untransfected neurons that differ with respect to their NL expression and that are therefore also likely to differ functionally with regard to synaptic transmission. Neurons with different NL expression levels in this type of mixed culture compete with each other for the same target neurons. Differences in the numbers of synapses formed by these neurons may then be secondary to differences in synaptic efficacy and synapse maintenance rather than caused by a genuine synaptogenic effect of NLs. The notion that the decrease in synapse density after knock-down of NLs in cultured neurons (Chih et al., 2005) may indeed be due to an activity-dependent homeostatic effect rather than an interference with a genuine synaptogenic role of NLs is supported by the fact that knock-down of NLs leads to a reduction in

the number of glutamatergic synapses without affecting the frequency or amplitude of spontaneous glutamatergic synaptic events. This finding indicates that knockdown of NLs in cultured neurons affects mainly labile and inactive synapses, which might even be unique to cultured neurons.

An alternative explanation for the discrepancy between the present data on NL 1-3 triple KOs and the data obtained after RNAi knock-down of NLs in cultured neurons (Chih et al., 2005) could be that off-target effects of the RNAi constructs cause perturbations of synapse stability. A recent publication showed that retraction of synapses and dendritic spines are induced by such off-target effects of RNAi (Alvarez et al., 2006). However, Chih et al. (2005) employed state-of-the-art RNAi control experiments in their study, and their findings are therefore very unlikely to be due to off-target artifacts.

It is also possible that the differences between the present study and the published cell culture experiments on NLs, which indicated that NL levels in neurons determine synapse densities (Chih et al., 2005; Dean et al., 2003; Graf et al., 2004; Levinson et al., 2005; Nam and Chen, 2005; Prange et al., 2004; Scheiffele et al., 2000), are due to specific compensatory effects in the NL 1-3 triple KOs in vivo, e.g., through upregulation of other cell adhesion systems. However, we regard this possibility to be unlikely for the following reasons. First, the expression of NL 4, which would be the ideal compensator of a loss of NLs 1-3, is not upregulated in NL 1-3- triple KOs (Table 1). Second, dramatic homeostatic compensatory changes in postsynaptic protein expression are also known to occur in cultured cells in vitro (Ehlers, 2003). If the loss of NLs in the triple KO mice were compensated by other synaptic cell adhesion processes, thus occluding an effect of NL deletion on synaptogenesis, the same compensatory mechanisms should be relevant in cultured neurons, because the time that typically passes between overexpression or knock-down of NLs and the subsequent analysis of cultured neurons (5–6 days) is similar to the time that passes between neurogenesis and synaptogenesis in the developing brain in utero. Likewise, functional redundancy among different synaptic cell adhesion systems is a rather unlikely explanation for the finding that the KO of NLs has no effect on synaptogenesis in the brain, while RNAi knock-down of NLs reduces synapse densities in cultured cells, because the same synaptic adhesion systems are likely to operate in the two preparations.

A final possibility that needs to be considered in the context of a possible role of NLs in synaptogenesis and in view of the discrepancies between our data on NL 1-3 triple KOs and the published literature on the putative synaptogenic function of NLs in cultured neurons is that the deletion of NLs in mice does not prevent initial synaptogenesis but rather delays it. While such an effect may have been missed in our analysis of synapse densities in the brainstem, which is almost mature at birth, analyses of the immature hippocampus of newborn NL 1-3 triple KO pups also failed to detect altered synapse densities (data not shown). These data indicate that even in early phases of synapse formation the lack of NLs does not affect synapse numbers in the intact brain.

NLs and Autism

Autism is a developmental disorder that is defined behaviorally by aberrant language acquisition, perturbed social interactions, and repetitive or ritualistic behaviors. Moreover, mental retardation and epilepsy are often associated with autism. The most consistent neuroanatomical finding in autistic patients is a tendency to unusually large brains with a disproportionate contribution of white matter to the increased brain volume (Herbert, 2005). In addition, functional abnormalities such as aberrant information processing or disturbed neuronal connectivity were postulated to contribute to the autistic phenotype (Herbert, 2005; Polleux and Lauder, 2004).

Studies on affected twins and the disproportionately high number of male patients with autism led to the consensus that autism is one of the most heritable psychiatric diseases. Indeed, loss-of-function mutations in the human NL genes *NLGN3* and *NLGN4* cause rare monogenic heritable forms of autism (Chih et al., 2004; Comoletti et al., 2004; Jamain et al., 2003; Laumonnier et al., 2004). Consequently, the NL 3 KO mice generated in the course of the present study could become a useful genetically defined animal model of autism. The phenotypic changes in NL triple KOs described here are compatible with current hypotheses about the functional deficiencies in the brains of autistic patients, according to which "*autism might be caused by an imbalance between excitation and inhibition in key neural systems*" (Polleux and Lauder, 2004). However, detailed behavioral analyses will be required to assess the extent to which NL 3 KO mice model the spectrum of behavioral and cognitive phenotypes that are typically associated with autism in humans.

Experimental Procedures

Absolute NL Protein Quantification

Brains from newborn and adult mice were homogenized in 320 mM sucrose, and protein concentrations were adjusted to a final concentration of 2 mg/ml. Defined amounts of GST-NL1, -NL2, -NL3, or -NL4 fusion proteins, including the epitopes of the isoform-specific antibodies to the different NLs, were run on SDS-PAGE gels in parallel with the brain homogenates. Fusion proteins and native NLs were detected on Western blots with isoform-specific polyclonal antibodies raised against 14 amino acid peptides, followed by an ^{125}I-labeled secondary antibody. After exposure to Biomax films (Kodak), bands were scanned and signal strength analyzed by densitometry (SIS).

In Situ Hybridization

Experiments were performed on paraformaldehyde-fixed 12 μm thick frontal and sagittal cryostat sections prepared from freshly frozen newborn and adult rat brains, respectively (Augustin et al., 1999). Antisense oligonucleotides representing bp 917–961 and 2822–2866 of rat NL 1, bp 550–594 and 2669–2713 of rat NL 2, bp 825–869, 2405–2449, and 2256–2300 of rat NL 3 were chosen as probes and labeled with terminal transferase by using ^{35}S-dATP (accession numbers: U22952, U41662, U41663, respectively). In control experiments, hybridizations were performed with a 1000-fold excess of the respective unlabeled oligonucleotide. Sections were exposed to Kodak Biomax film for 2 weeks. Different oligonucleotides for a given NL isoform gave identical labeling patterns.

Protein Quantification

NL 1-3 triple KO brains and brains from mice of a wild-type line with the same mosaic genetic background, which was derived from NL 1-3 triple KO interbreedings, were collected and immediately frozen in liquid nitrogen. Brains of the selected genotypes were

homogeneized in 320 mM sucrose and adjusted to a final protein concentration of 2 mg/ml. 20 μl per lane were run on SDS-PAGE gels and blotted onto nitrocellulose membranes. Several proteins (Table 1) were detected with specific primary antibodies and fluorescently labeled secondary antibodies and quantified on an Odyssey fluorescence reader (Li-Cor). Each blot was stained in parallel for a reference protein (actin or tubulin) and protein levels were expressed as the ratio over the reference protein.

Immunostaining and Light Microscopic Quantification

Brains from newborn control and NL 1-3 triple KO pups were removed and either frozen by immersion in N_2-cooled isopentane at −40°C or immersion-fixed overnight in 4% paraformaldehyde, cryoprotected in sucrose, and frozen on dry ice. Serial frontal cryostat sections (12 μm thick) were collected on slides. Sections from freshly frozen brains were further fixed by immersion in 4% paraformaldehyde at 4°C or in −20°C cooled methanol for 10 min. After blocking, paraformaldehyde-fixed sections were stained for VIAAT, VGluT1/2 (all guinea-pig, 1:3000 and 1:8000 or 1:10,000, Chemicon), and synaptophysin 1 (1:1000, SIGMA). Methanol-fixed sections were stained for $GABA_AR$ α1 (1:20,000, J.M. Fritschy), gephyrin (1:2000, Synaptic Systems), and GlyRα1 (1:100, Synaptic Systems) or PSD-95 (1:1000, Antibodies Inc.), VIAAT (rabbit, 1:4000, Chemicon), and VGluT1/2. All images were acquired as single layers at a zoom factor 4 using a Zeiss inverted confocal laser scanning microscope (LSM 510) with a 63× oil-immersion lens. For quantitative analyses (Figures 6 and 7), the gain and offset were held constant across images to allow for intensity comparisons. Images were then imported into the AnalySIS software (Soft-Imaging Systems) and puncta were quantified. For quantifications, thresholds were manually determined for each image prior to binarization, followed by a particle separation filter. The resulting image was added to the original, and a particle detection was carried out to measure particle number, area, mean intensity, and integral intensity.

Neurons were prepared from P0 hippocampi and cultured as described (Dresbach et al., 2004). Neurons at DIV 21 were fixed with 4% paraformaldehyde (15 min on ice), thoroughly washed in PB, and further stained for synapsin (rabbit, 1:2000, Synaptic Systems) and PSD-95 (mouse, 1:1000, Antibodies Inc.). Coverslips were observed at high magnification (100×) with an upright epifluorescence Olympus BX-61 microscope. Images were acquired with a digital camera (F-View II) and analyzed with the AnalySIS software (Soft-Imaging Systems). Labeled puncta were quantified by touch-count analysis on portions of dendrites of comparable diameter.

Ultrastructural Analyses

Brains from newborn wild-type and NL 1-3 triple KO pups were fixed by immersion in 4% paraformaldehyde/0.1% glutaraldehyde in 0.1 M phosphate buffer. 400 μm thick vibratome sections of the brainstem were collected, washed, osmicated for 1 hr (1% OsO_4 in phosphate buffer), dehydrated through a graded series of ethanol and propylene oxide, and embedded in Durcupan (Durcupan ACM, Fluka) by a 48 hr polymerization at 60°C. Light gold ultrathin sections were cut, contrasted with uranyl acetate and lead citrate, and observed in a LEO 912AB transmission electron microscope (Zeiss). Digital images were captured with a ProScan CCD camera and analyzed with the Analysis software (Soft Imaging System).

Electrophysiological Recordings in Dissociated Cortical Neurons

Cocultures of neocortical explants and dissociated neocortical target neurons of newborn NL 1-3 triple KOs and triple heterozygous littermates were prepared as described (Mohrmann et al., 1999). After 2 weeks in vitro, recordings were performed in neurons from NL1-3 triple KO and triple heterozygous animals. AMPA receptor-mediated miniature postsynaptic currents (AMPA mPSCs) were recorded at −60 mV holding potential in the presence of 1 mM Mg^{2+}, 20 μM bicuculline methochloride, and 1 μM TTX. To increase the frequency of AMPA mPSCs an elevated K^+ concentration (35 mM) in the extracellular solution was used. Glutamate receptor-mediated PSCs were evoked by local extracellular stimulation using wide-tip patch pipettes as stimulating electrodes and were recorded at −60 mV holding potential. Evoked NMDA and AMPA receptor-mediated PSCs were pharmacologically isolated using DNQX and D-AP5, respectively. Extracellular solutions were switched during the experiment using a whole-cell superfusion system.

Ventilation Recordings

Ventilation patterns were recorded by whole-body plethysmography, where unanesthetized newborn pups were placed in a 15 ml closed chamber connected to a differential pressure transducer (CD15 Carrier Demodulator, ValiDyne). The analog signal of ventilation-related changes of air pressure was amplified and digitized using an A/D-converter (DigiData 3200, Axon Instruments) and analyzed using commercially available AxoTape and AxoGraph software (Axon Instruments).

Electrophysiological Recordings in Brainstem Slices

All electrophysiological analyses were performed on brainstem neurons of mice whose genotype was unknown to the experimenter. Acute slices containing the pre-Bötzinger complex (PBC) and hypoglossal nucleus (NH) from newborn littermate mice were used for whole-cell recordings. The bath solution in all experiments consisted of (in mM) 118 NaCl, 3 KCl, 1.5 $CaCl_2$, 1 $MgCl_2$, 25 $NaHCO_3$, 1 NaH_2PO_4, 5 glucose, pH 7.4, aerated with 95% O_2 and 5% CO_2 and kept at 28°C–30°C. Evoked glutamatergic and GABAergic/glycinergic PSCs were recorded from hypoglossal neurons in the presence of 1 μM strychnine and 1 μM bicuculline or 10 μM CNQX, respectively. PSCs were evoked by 0.1 Hz field stimulations of axons of interneurons close to the PBC using a bipolar platinum electrode. An isolation unit IsoFlex (A.M.P.I.) with a custom-built power supply was used to apply currents of supramaximal stimulation strength (around 1 mA actual current near the slice as confirmed by current measurements). The pipette solution for evoked glutamatergic and GABAergic/glycinergic PSCs measurements contained (in mM) 140 Kgluconate (glutamatergic PSCs) or 140 KCl (GABAergic/glycinergic PSCs), 1 $CaCl_2$, 10 EGTA, 2 $MgCl_2$, 4 Na_3ATP, 0.5 Na_3GTP, 10 HEPES, pH 7.3. Peak amplitudes were averaged from 25 consecutive responses. To monitor changes in input resistance, current responses to a −10 mV voltage step (20 ms) from a holding potential of −70 mV were recorded before every fifth stimulus. In all experiments the distance between the stimulation and recording electrodes was similar between slices of different genotypes. Spontaneous GABAergic/glycinergic and glutamatergic PSCs were recorded from neurons of the PBC at a Cl^- reversal potential of about 0 mV in 10 μM CNQX or 1 μM strychnine and 1 μM bicuculline, respectively. Signals with amplitudes of at least two times above background noise were selected, and statistical significance was tested in each experiment. Spontaneous miniature GABAergic/glycinergic and glutamatergic PSCs were recorded as described above, but in the presence of 0.5 μM tetrodotoxin (TTX). Signals with amplitudes of at least two times above background noise were selected, and statistical significance was tested in each experiment. There were no significant differences in noise levels between different genotypes. Voltage-activated currents were measured from neurons of the PBC with patch electrodes containing (in mM) 110 $CsCl_2$, 30 TEA-Cl (for Na^+ and Ca^{2+}-current), or 140 KCl (for K^+ current); 1 $CaCl_2$, 10 EGTA, 2 $MgCl_2$, 4 Na_3ATP, 0.5 Na_3GTP, 10 HEPES, pH 7.3, and with 0.5 μM tetrodotoxin and 200 μM Cd^{2+} for blocking Na^+ and Ca^{2+} current in the bath solution. After establishing the whole-cell configuration, membrane capacitance serial and membrane resistances were estimated from current transient induced by 20 mV hyperpolarization voltage commands from a holding potential of −70 mV. The serial resistance was compensated by 80%, and patches with a serial resistance of >20 MΩ, a membrane resistance of <0.8 GΩ, or leak currrents of >150 pA were excluded. The membrane currents were filtered by a four-pole Bessel filter at a corner frequency of 2 kHz, and digitized at a sampling rate of 5 kHz using the DigiData 1200B interface (Axon Instruments). Currents were recorded and quantified as peak currents in response to voltage steps from −70 mV to 0 mV. The current measurements were corrected using the P/4 protocol that subtracts leak currents measured during four leak-subtraction prepulses applied immediately before each voltage step. Data acquisition and analysis was done using commercially available software (pClamp 6.0 and AxoGraph 4.6, Axon Instruments, and Prism 4 Software, GraphPad).

Supplemental Data

The Supplemental Data for this article, including four Figures, can be found online at http://www.neuron.org/cgi/content/full/51/6/741/DC1/.

Acknowledgments

This work was supported by a postdoctoral fellowship and institutional support from the Max-Planck-Society (N.B.), by grants BR1107/3 and BR1107/4 from the German Research Foundation (N.B), by grant FZT103 from the German Research Foundation Center for Molecular Physiology of the Brain (N.B., W.Z.), by a postdoctoral fellowship of the German Research Foundation (M.M.), by grant R37 MH52804-08 from the National Institute of Mental Health (T.C.S.), and by the Howard Hughes Medical Institute (T.C.S.). We thank Guido Meyer (Max Planck Institute of Experimental Medicine, Göttingen) for helpful discussions, and Klaus Hellmann (Max Planck Institute of Experimental Medicine, Göttingen), Iza Kornblum, Andrea Roth, Eva Borowicz (all University of Texas Southwestern Medical Center, Dallas), and the staff of the DNA Core Facility and the Transgenic Animal Facility of the Max Planck Institute of Experimental Medicine (Göttingen) for excellent technical assistance. We are grateful to Jean-Marc Fritschy (University of Zürich) for generously providing anti-$GABA_A$-receptor antibodies.

Received: January 30, 2006
Revised: July 31, 2006
Accepted: September 1, 2006
Published: September 20, 2006

References

Alvarez, V.A., Ridenour, D.A., and Sabatini, B.L. (2006). Retraction of synapses and dendritic spines induced by off-target effects of RNA interference. J. Neurosci. *26*, 7820–7825.

Augustin, I., Betz, A., Herrmann, C., Jo, T., and Brose, N. (1999). Differential expression of two novel Munc13 proteins in rat brain. Biochem. J. *337*, 363–371.

Biederer, T., and Südhof, T.C. (2000). Mints as adaptors. Direct binding to neurexins and recruitment of munc18. J. Biol. Chem. *275*, 39803–39806.

Boucard, A.A., Chubykin, A.A., Comoletti, D., Taylor, P., and Südhof, T.C. (2005). A splice code for trans-synaptic cell adhesion mediated by binding of neuroligin 1 to alpha- and beta-neurexins. Neuron *48*, 229–236.

Chih, B., Afridi, S.K., Clark, L., and Scheiffele, P. (2004). Disorder-associated mutations lead to functional inactivation of neuroligins. Hum. Mol. Genet. *13*, 1471–1477.

Chih, B., Engelman, H., and Scheiffele, P. (2005). Control of excitatory and inhibitory synapse formation by neuroligins. Science *307*, 1324–1328.

Chih, B., Gollan, L., and Scheiffele, P. (2006). Alternative splicing controls selective trans-synaptic interactions of the neuroligin-neurexin complex. Neuron *51*, 171–178.

Chubykin, A.A., Liu, X., Comoletti, D., Tsigelny, I., Taylor, P., and Südhof, T.C. (2005). Dissection of synapse induction by neuroligins: Effects of a neuroligin mutation associated with autism. J. Biol. Chem. *280*, 22365–22374.

Comoletti, D., De Jaco, A., Jennings, L.L., Flynn, R.E., Gaietta, G., Tsigelny, I., Ellisman, M.H., and Taylor, P. (2004). The Arg451Cys-neuroligin-3 mutation associated with autism reveals a defect in protein processing. J. Neurosci. *24*, 4889–4893.

Dean, C., Scholl, F.G., Choih, J., DeMaria, S., Berger, J., Isacoff, E., and Scheiffele, P. (2003). Neurexin mediates the assembly of presynaptic terminals. Nat. Neurosci. *6*, 708–716.

Dresbach, T., Neeb, A., Meyer, G., Gundelfinger, E.D., and Brose, N. (2004). Synaptic targeting of neuroligin is independent of neurexin and SAP90/PSD95 binding. Mol. Cell. Neurosci. *27*, 227–235.

Ehlers, M.D. (2003). Activity level controls postsynaptic composition and signaling via the ubiquitin-proteasome system. Nat. Neurosci. *6*, 231–242.

El-Husseini, A., Schnell, E., Dakoji, S., Sweeney, N., Zhou, Q., Prange, O., Gauthier-Campbell, C., Aguilera-Moreno, A., Nicoll, R.A., and Bredt, D.S. (2002). Synaptic strength regulated by palmitate cycling on PSD-95. Cell *108*, 849–863.

Fu, Z., Washbourne, P., Ortinski, P., and Vicini, S. (2003). Functional excitatory synapses in HEK293 cells expressing neuroligin and glutamate receptors. J. Neurophysiol. *90*, 3950–3957.

Fukata, Y., Tzingounis, A.V., Trinidad, J.C., Fukata, M., Burlingame, A.L., Nicoll, R.A., and Bredt, D.S. (2005). Molecular constituents of neuronal AMPA receptors. J. Cell Biol. *169*, 399–404.

Garner, C.C., Zhai, R.G., Gundelfinger, E.D., and Ziv, N.E. (2002). Molecular mechanisms of CNS synaptogenesis. Trends Neurosci. *25*, 243–251.

Graf, E.R., Zhang, X., Jin, S.X., Linhoff, M.W., and Craig, A.M. (2004). Neurexins induce differentiation of GABA and glutamate postsynaptic specializations via neuroligins. Cell *119*, 1013–1026.

Hata, Y., Butz, S., and Südhof, T.C. (1996). CASK: a novel dlg/PSD95 homolog with an N-terminal calmodulin-dependent protein kinase domain identified by interaction with neurexins. J. Neurosci. *16*, 2488–2494.

Herbert, M.R. (2005). Large brains in autism: the challenge of pervasive abnormality. Neuroscientist *11*, 417–440.

Hirao, K., Hata, Y., Ide, N., Takeuchi, M., Irie, M., Yao, I., Deguchi, M., Toyoda, A., Südhof, T.C., and Takai, Y. (1998). A novel multiple PDZ domain-containing molecule interacting with N-methyl-D-aspartate receptors and neuronal cell adhesion proteins. J. Biol. Chem. *273*, 21105–21110.

Ichtchenko, K., Hata, Y., Nguyen, T., Ullrich, B., Missler, M., Moomaw, C., and Südhof, T.C. (1995). Neuroligin 1: a splice site-specific ligand for beta-neurexins. Cell *81*, 435–443.

Ichtchenko, K., Nguyen, T., and Südhof, T.C. (1996). Structures, alternative splicing, and neurexin binding of multiple neuroligins. J. Biol. Chem. *271*, 2676–2682.

Irie, M., Hata, Y., Takeuchi, M., Ichtchenko, K., Toyoda, A., Hirao, K., Takai, Y., Rosahl, T.W., and Südhof, T.C. (1997). Binding of neuroligins to PSD-95. Science *277*, 1511–1515.

Jamain, S., Quach, H., Betancur, C., Rastam, M., Colineaux, C., Gillberg, I.C., Soderstrom, H., Giros, B., Leboyer, M., Gillberg, C., and Bourgeron, T. (2003). Mutations of the X-linked genes encoding neuroligins NLGN3 and NLGN4 are associated with autism. Nat. Genet. *34*, 27–29.

Kim, E., and Sheng, M. (2004). PDZ domain proteins of synapses. Nat. Rev. Neurosci. *5*, 771–781.

Kim, E., Niethammer, M., Rothschild, A., Jan, Y.N., and Sheng, M. (1995). Clustering of Shaker-type K^+ channels by interaction with a family of membrane-associated guanylate kinases. Nature *378*, 85–88.

Kornau, H.C., Schenker, L.T., Kennedy, M.B., and Seeburg, P.H. (1995). Domain interaction between NMDA receptor subunits and the postsynaptic density protein PSD-95. Science *269*, 1737–1740.

Laumonnier, F., Bonnet-Brilhault, F., Gomot, M., Blanc, R., David, A., Moizard, M.P., Raynaud, M., Ronce, N., Lemonnier, E., Calvas, P., et al. (2004). X-linked mental retardation and autism are associated with a mutation in the NLGN4 gene, a member of the neuroligin family. Am. J. Hum. Genet. *74*, 552–557.

Levinson, J.N., Chery, N., Huang, K., Wong, T.P., Gerrow, K., Kang, R., Prange, O., Wang, Y.T., and El-Husseini, A. (2005). Neuroligins mediate excitatory and inhibitory synapse formation: involvement of PSD-95 and neurexin-1beta in neuroligin-induced synaptic specificity. J. Biol. Chem. *280*, 17312–17319.

Li, Z., and Sheng, M. (2003). Some assembly required: the development of neuronal synapses. Nat. Rev. Mol. Cell Biol. *4*, 833–841.

McMahon, H.T., Bolshakov, V.Y., Janz, R., Hammer, R.E., Siegelbaum, S.A., and Südhof, T.C. (1996). Synaptophysin, a major synaptic vesicle protein, is not essential for neurotransmitter release. Proc. Natl. Acad. Sci. USA *93*, 4760–4764.

Meyer, G., Varoqueaux, F., Neeb, A., Oschlies, M., and Brose, N. (2004). The complexity of PDZ domain-mediated interactions at glutamatergic synapses: a case study on neuroligin. Neuropharmacology *47*, 724–733.

Missler, M., Zhang, W., Rohlmann, A., Kattenstroth, G., Hammer, R.E., Gottmann, K., and Südhof, T.C. (2003). Alpha-neurexins couple Ca^{2+} channels to synaptic vesicle exocytosis. Nature *423*, 939–948.

Mohrmann, R., Werner, M., Hatt, H., and Gottmann, K. (1999). Target-specific factors regulate the formation of glutamatergic transmitter release sites in cultured neocortical neurons. J. Neurosci. *19*, 10004–10013.

Montgomery, J.M., Zamorano, P.L., and Garner, C.C. (2004). MAGUKs in synapse assembly and function: an emerging view. Cell. Mol. Life Sci. *61*, 911–929.

Nam, C.I., and Chen, L. (2005). Postsynaptic assembly induced by neurexin-neuroligin interaction and neurotransmitter. Proc. Natl. Acad. Sci. USA *102*, 6137–6142.

Polleux, F., and Lauder, J.M. (2004). Toward a developmental neurobiology of autism. Ment. Retard. Dev. Disabil. Res. Rev. *10*, 303–317.

Prange, O., Wong, T.P., Gerrow, K., Wang, Y.T., and El-Husseini, A. (2004). A balance between excitatory and inhibitory synapses is controlled by PSD-95 and neuroligin. Proc. Natl. Acad. Sci. USA *101*, 13915–13920.

Ritter, B., and Zhang, W. (2000). Early postnatal maturation of $GABA_A$-mediated inhibition in the brainstem respiratory rhythm-generating network of the mouse. Eur. J. Neurosci. *12*, 2975–2984.

Scheiffele, P. (2003). Cell-cell signaling during synapse formation in the CNS. Annu. Rev. Neurosci. *26*, 485–508.

Scheiffele, P., Fan, J., Choih, J., Fetter, R., and Serafini, T. (2000). Neuroligin expressed in nonneuronal cells triggers presynaptic development in contacting axons. Cell *101*, 657–669.

Schnell, E., Sizemore, M., Karimzadegan, S., Chen, L., Bredt, D.S., and Nicoll, R.A. (2002). Direct interactions between PSD-95 and stargazin control synaptic AMPA receptor number. Proc. Natl. Acad. Sci. USA *99*, 13902–13907.

Serafini, T. (1999). Finding a partner in a crowd: neuronal diversity and synaptogenesis. Cell *98*, 133–136.

Song, J.Y., Ichtchenko, K., Südhof, T.C., and Brose, N. (1999). Neuroligin 1 is a postsynaptic cell-adhesion molecule of excitatory synapses. Proc. Natl. Acad. Sci. USA *96*, 1100–1105.

Sperry, R.W. (1963). Chemoaffinity in the orderly growth of nerve fiber patterns and connections. Proc. Natl. Acad. Sci. USA *50*, 703–710.

Talebizadeh, Z., Lam, D.Y., Theodoro, M.F., Bittel, D.C., Lushington, G.H., and Butler, M.G. (2006). Novel splice isoforms for NLGN3 and NLGN4 with possible implications in autism. J. Med. Genet. *43*, e21.

Tarsa, L., and Goda, Y. (2002). Synaptophysin regulates activity-dependent synapse formation in cultured hippocampal neurons. Proc. Natl. Acad. Sci. USA *99*, 1012–1016.

Turrigiano, G.G., and Nelson, S.B. (2004). Homeostatic plasticity in the developing nervous system. Nat. Rev. Neurosci. *5*, 97–107.

Varoqueaux, F., Jamain, S., and Brose, N. (2004). Neuroligin 2 is exclusively localized to inhibitory synapses. Eur. J. Cell Biol. *83*, 449–456.

Yamagata, M., Sanes, J.R., and Weiner, J.A. (2003). Synaptic adhesion molecules. Curr. Opin. Cell Biol. *15*, 621–632.

Zhang, W., Rohlmann, A., Sargsyan, V., Aramuni, G., Hammer, R.E., Südhof, T.C., and Missler, M. (2005). Extracellular domains of alpha-neurexins participate in regulating synaptic transmission by selectively affecting N- and P/Q-type Ca^{2+} channels. J. Neurosci. *25*, 4330–4342.